European Journal of Clinical Pharmacy
Print ISSN: 2385-409X, **Online ISSN**: 3105-0409
Website: https://farmclin.com/

SYNTHESIS AND CHARACTERIZATION OF 2-[(4-HYDROXY-3-METHOXY-PHENYL)-MORPHOLIN-4-YL-METHYL]-BENZO[DE]ISOQUINOLINE-1,3-DIONE AND EVALUATION OF ITS INHIBITION POTENTIAL AGAINST MILD STEEL IN 1.0 M HCl SOLUTION

Article History:

Name of Author:
G. Banu Karthi[1], R. Baranika[1], M. Yosuva Suvaikin[2]

Affiliation: *[1]PG and Research Department of Chemistry, Jamal Mohamed College (Autonomous), Affiliated to Bharathidasan University, Tiruchirappalli 620 020, Tamil Nadu, India*
[2] Department of Chemistry, H.H. The Rajah's College, Pudukkottai 622 001, Tamil Nadu, India

Corresponding Author:

Received: 21-11-2025
Revised: 29-11-2025
Accepted: 16-12-2025
Published: 20-12-2025

Abstract: Background: Mild steel corrosion in acid medium challenges the industries greatly increasing the need for eco-friendly and efficient inhibitors. In this work 2-[(4-hydroxy-3-methoxy-phenyl)-morpholin-4-yl-methyl]-benzo[de]isoquinoline-1,3-dione (MVN), a new Mannich base was prepared and tested for its effectiveness to inhibit corrosion in 1.0 M HCl. NMR, FT-IR, UV-Visible and mass spectroscopic evidences confirmed its structure. Analysis including weight loss, electrochemical impedance spectroscopy (EIS) and potentio-dynamic polarization assessed its inhibition performance against corrosion. The inhibition efficiency elevated with increase in concentration and it was found to be 95 % at 10-3 M. Decrease in the corrosion current density and an increment in charge transfer resistance as reported in the electrochemical studies revealed a protective film on the surface of the metal. Temkin's isotherm studies, ΔG° = -34.37 KJ mol-1 predicted a mixed physisorption and chemisorption. Increased adsorption due to the presence of π-electrons and heteroatoms. The energy gap between the HOMO and LUMO orbitals of MVN is 3.12 eV (DFT analysis). Also, MEP mapping revealed electron-rich N and O atoms as active adsorption sites. These findings demonstrate that MVN is an effective corrosion inhibitor for mild steel in acidic medium.

Keywords: Mild steel corrosion; Acidic medium (HCl); Mannich base inhibitor; Electrochemical impedance spectroscopy (EIS); Potentiodynamic polarization; Adsorption isotherm (Temkin); Corrosion inhibition efficiency; Density Functional Theory (DFT); Molecular electrostatic potential (MEP); Mixed adsorption mechanism.

INTRODUCTION

Corrosion is a well-known unavailable reaction

implying disintegration of metals owing to interactions (electrochemical or chemical) with its surroundings. In all known engineering materials, mild steel is recommended in most industries like petroleum refining, construction and chemical processing due to the lesser cost, easy fabricability and higher strength. But in industrial processes including acid cleaning, pickling, oil well acidizing and descaling, mild steel is prone to corrosion owing to violent acidic environments (Evans & Kim, 2001; Pedeferri, 2018). The vulnerability causes decrease in material lifespan, potential safety hazards and economic losses promising corrosion control as a main criterion for industrial and scientific research (Jones, 1996).

3-4 % of the GDP (Gross Domestic Product) – total economic value, among industrialized nations is because of corrosion (Koch et al., 2005). Together with the financial losses, the operational reliability and environmental safety are also affected by corrosion. The contemporary research highlights corrosion as a major challenge globally demanding evolution of sustainable and modern mitigation policies (Kumar et al., 2024). Hence, enormous protocols have been devised to minimize corrosion by alloying, protective coatings, use of corrosion inhibitors and cathodic protection. Amidst these, use of corrosion inhibitors is known as one of the best cost-efficient methods, specially in acidic conditions (Quraishi & Jamal, 2001).

Corrosion inhibitors when added in minor quantities, prevalently decrease the degradation rate in metal. Of the many inhibitors, organic inhibitors have achieved greater attraction because of their potential to adsorb onto metal surfaces thereby achieving a protective film which isolates the metal from that of the corrosive medium (Bentiss et al., 2000). For any inhibitor to be highly effective, the conditions like molecular structure, especially the availability of heteroatoms like oxygen, nitrogen and sulphur together with functional groups with π-electron groups are essential (Ebenso, 2003; Popova, 2007). The mechanism for adsorption may be physisorption or chemisorption or a process combining both of them.

In the present years, concern for health and environment is related with the traditional inorganic inhibitors like phosphates and chromates leading the aggravating desire in eco-friendly alternatives (Raja & Sethuraman, 2008). Recent research highlights the advancement of green corrosion inhibitors, inclusive of ionic liquids, plant extracts and hybrid organic systems offering decrease in toxicity and increase in sustainability (Emmanuel, 2024; Mobin et al., 2023). Moreover, organic molecules having conjugated systems, aromatic rings and electron-donating functional groups have established enhanced inhibition efficiency owing to potentials including film-forming abilities and strong adsorption capabilities (Al-Amiery et al., 2022; Verma et al., 2016).

Of the different divisions of organic inhibitors Mannich bases have proved to be the greatly efficient corrosion inhibitors. These bases are prepared by the condensation of an amine, an aldehyde and an active hydrogen-owning compound, yielding a compound with several adsorption centres. The availability of conjugated π-systems and heteroatoms promotes the influence with metal surfaces in reduction of corrosion rates (Al-Amiery et al., 2022). The adsorption strength and the electron-donating ability are improved with the presence of functional groups like -OH, -OCH3, and -NH (Ju et al., 2008). Accordingly, the current studies have disclosed that the Mannich-base derivatives may attain an inhibition efficiency up to 95-99 % in acidic medium owing to the mixed inhibition mechanism and its strong adsorption (Liu et al., 2026). Also, the present-day reviews showcase that the improved Mannich bases are the suitable corrosion inhibitors in several industrial applications (Dwivedi et al., 2021).

As morpholine-based Mannich bases have fascinated awareness because of their increased performance in inhibition. The inclusion of morpholine provides oxygen and nitrogen atoms, which enables coordination with metal surfaces and enhance the efficiency towards adsorption (Singh & Quraishi, 2010). Like-wise, vanillin-associated compounds, having methoxy and hydroxyl functional groups, grant enhancement in inhibition performance owing to increment of electron density and the potential to generate constant interactions with metal surfaces (Eddy et al., 2010). These structural modifications become the reason for such compounds (Mannich bases) to serve as corrosion inhibitors.

Though, there has been significant progress, requirement for highly efficient, cost-effective and environmentally benign inhibitors is very high. In this regard, this study well-defines the synthesis and characterization of a new Mannich base, 2-[(4-hydroxy-3-methoxy-phenyl)-morpholin-4-yl-methyl]-benzo[de]isoquinoline-1,3-dione (MVN), and its evaluation as a corrosion inhibitor for mild steel in 1.0 M HCl solution. The compound is synthesized and it has multiple active sites like π-electron systems and heteroatoms, enhancing the adsorption and thereby the inhibition efficiency.

Evaluation of the performance towards inhibition of corrosion in the novel compound (MVN) was by electrochemical techniques (Electrochemical Impedance Spectroscopy and potentiodynamic polarization) and weight-loss measurements. Also, with the help of the suitable adsorption isotherms, the adsorption behaviour was predicted in order to develop the mechanism of inhibition. This investigation turns out to develop highly sustainable, effective and high-performance corrosion inhibitors

for industrial requirements.

Also, DFT calculations were employed to understand the electronic properties and adsorption behavior of MVN. Parameters such as HOMO, LUMO, ΔE, and MEP provide insight into corrosion inhibition mechanisms (Moradi et al., 2011; Politzer & Murray, 2002).

Materials and Methods

Materials and Specimen Preparation

Mild steel specimens of the composition (wt %) C (0.07), S (0.00), P (0.008), Mn (0.34), and Fe (remaining) were used. For the weight loss measurements, rectangular strips (4 × 1 × 0.025 cm) and, cylindrical rods covered with PTFE (polytetrafluoroethylene) with surface area of 1 cm^2 exposed serves as the working electrode for the purpose of electrochemical studies. To start with, before any experiment, mechanical polishing of specimens with emery papers (successive grades), rinsing with distilled water, degreasing with the aid of acetone, and drying is done (El Ibrahimi & Berdimurodov, 2023). From the analytical grade concentrated HCl (12 M), the required dilutions of HCl solution were prepared with distilled water. These solutions were newly prepared, and experiments were performed under magnetically stirred conditions (BRIAN S FURNIS, 2020).**2**

Synthesis of the Ligand

The ligand, 2-[(4-hydroxy-3-methoxyphenyl)-morpholin-4-yl-methyl]-benzo[de]isoquinoline-1,3-dione (MVN) (Figure 1), was prepared by the Mannich condensation reaction. Nicotinamide was dissolved in ethanol (10 mL), to this solution morpholine was added under ice-cold conditions. Following it, Vanillin was added in drops with continuous stirring. All the above reagents were of uniform concentrations (0.01 mol). For an approximate duration of 5 days, the above reaction mixture was kept undisturbed at room temperature. The precipitate formed as such was washed with distilled water and CCl_4 after filtration. Then it was dried and recrystallized from ethanol (m.p. 180 °C). The purity check was performed both with elemental analysis and thin-layer chromatography (Smith, 2025).

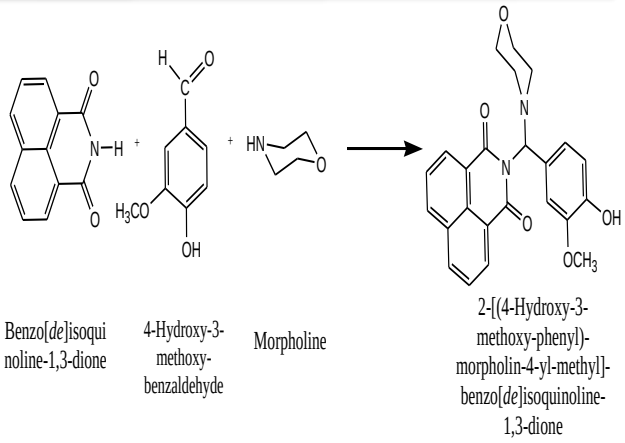

Figure 1. Preparation of MVN

Characterization Techniques

Electronic absorption spectra were observed in DMF solution using a PerkinElmer EZ 301 double-beam UV-Visible spectrophotometer in the range 190-1100 nm (Skoog et al., 2007). Functional group analysis was performed using a PerkinElmer Spectrum-1 FT-IR spectrometer (Silverstein et al., 2005). ^1H and ^{13}C NMR spectra were recorded on JEOL 400 MHz spectrometers using DMSO-d_6 (solvent) and tetramethylsilane (internal reference) (Pavia et al., 2001). Mass spectral information were detected with JEOL D-300 and SX-102 instruments in electron impact (EI) mode to find the fragmentation patterns and the molecular weight (Watson & Sparkman, 2007).

Preparation of Inhibitor Solutions

MVN stock solution (10^{-3} M) was made with methanol. Suitable series of test solutions of varying dilutions in the range of 10^{-4} to 10^{-7} M were obtained. All the above solutions were newly prepared before use (Elachouri et al., 1996).

Weight Loss Measurements

The mild steel specimens were pre-weighed and then immersed in 100 mL of 1.0 M HCl solution at 303 ± 1 K for gravimetric measurements both the presence of MVN (various concentrations) and its absence. At the end of the allotted time of immersion, the mild steel specimens were removed from the acid solution. It was then washed, dried, and reweighed. Each experiment was triplicated, and the average values were observed (Ebenso, 2003; Quraishi & Rawat, 2001).

The inhibition efficiency (IE%) and surface coverage (θ) were evaluated from the equation:

$$\theta = \frac{W_0 - W_1}{W_0}$$

$$\text{I. E. (\%)} = \frac{W_0 - W_1}{W_0} \times 100$$

Where, W_1, and W_0 are the weight loss value

in presence and absence of inhibitors, respectively.

Electrochemical Measurements

Electrochemical experiments done with Princeton Applied Research electrochemical analyzer using conventional three-electrode system having mild steel as the working electrode, platinum foil as the counter electrode, and a saturated calomel electrode (SCE) as the reference electrode. Potentiodynamic polarization curves were recorded at a scan rate of 1 mV s^{-1}, starting from −0.2 V with respect to the open circuit potential (Mansfeld, 1990; Stern & Geary, 1957). Electrochemical impedance spectroscopy (EIS) measurements were performed at open circuit potential over a frequency range of 100 kHz to 0.1 Hz with an AC amplitude of 10 mV (Macdonald, 2006).

Adsorption Studies

The standard free energy of adsorption ($\Delta G°_{a}d_{s}$) was calculated using the following relation: $\Delta G° = -RT \ln (K \times 55.5)$ KJ/mole., where (T) is the absolute temperature, (R) is the universal gas constant, , and (K) is the adsorption equilibrium constant, determined from: $K = \theta\,(C/1-\theta)$, where (θ) is the surface coverage and (C) is the inhibitor concentration (Langmuir, 1918).

DFT Calculations

The optimized structure, HOMO–LUMO energies, and energy gap (ΔE) were obtained using DFT. MEP analysis was performed to identify active adsorption sites.

Results and Discussion

3.1 Spectral Characterization of MVN

3.1.1 UV-Visible Analysis

The UV-Visible spectrum of MVN (Figure 2) recorded in DMSO shows absorption bands at 209.5, 226.7, 276.2, 312.1, and 372.8 nm. The intense bands at 209.5 and 226.7 nm are due to the π→π* transitions of the aromatic system, predicting extended conjugation. At 276.2 and 312.1 nm, the bands are seen owing to the n→π* transitions associated with heteroatoms (N and O) and carbonyl groups. The peak observed at 372.8 nm corresponds to the intramolecular charge transfer (ICT), showing good electron delocalization inside the molecule. Altogether, the presence of a conjugated system containing heteroatoms is confirmed and it is consistent with the proposed structure.

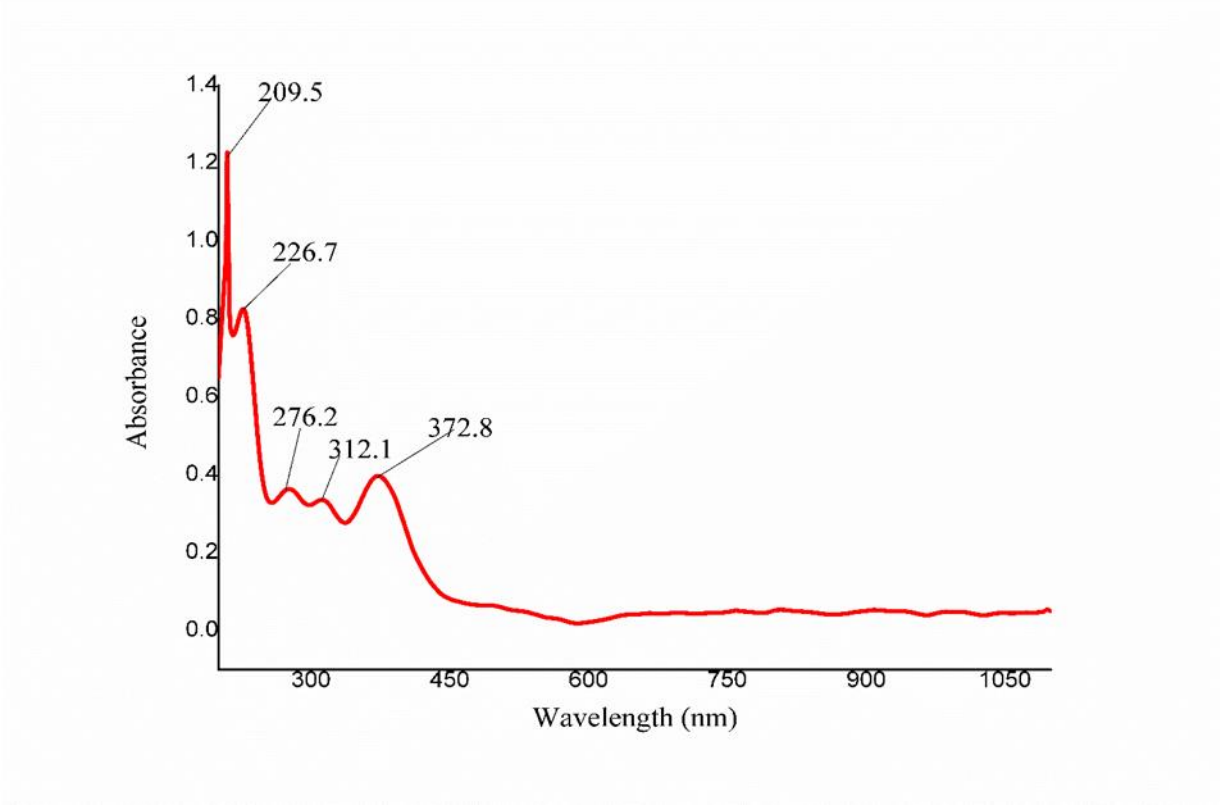

Figure 2. UV-Vis Spectrum of MVN

3.1.2 FT-IR Analysis

The FT-IR spectrum (4000-450 cm^{-1}) predicts the formation of MVN (Figure 3). The characteristic C–N–C stretching vibrations observed at 1259, 1224, and 1204 cm^{-1} indicates successful Mannich condensation. Aromatic and aliphatic C–H stretching bands appearing approximately at 3050 cm^{-1} and 2946-2839 cm^{-1}, respectively, speaks about the

occurrence of both aromatic rings and methylene bridges. At 1632 cm^{-1}, there appears a strong peak corresponding to the C=O stretching, predicting the retention of carbonyl functionality. Furthermore, the appearance of peaks at 1122 and 1142 cm^{-1} (C–N stretching bands) further confirms the presence of morpholine moiety. Vibrations (Out-of-plane C–H bending) in the range 872-756 cm^{-1} affirms the integrity of the aromatic system. Overall, the spectral shifts and new bands validate the successful formation of the Mannich base structure.

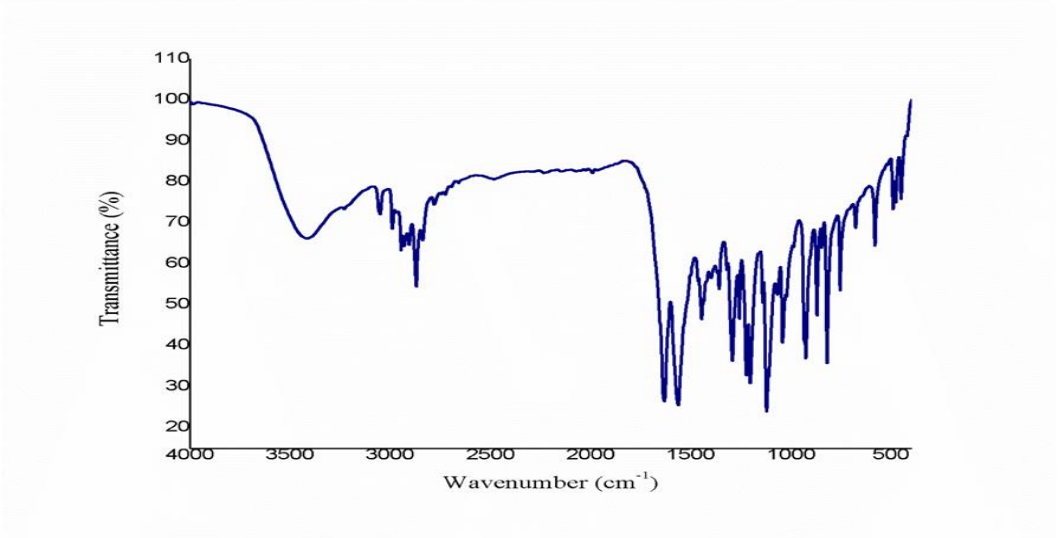

Figure 3. FT-IR Spectrum of MVN

3.1.3 NMR Analysis

The ^1H NMR spectrum in DMSO-d_6 gives suitable signals confirming the molecular structure (Figure 4). The multiplets appearing at δ 6.5-8.5 ppm implies the aromatic protons. The singlet, around δ 9.0-0.0 ppm (downfield) is attributes to the –NH proton, convincing the presence of an amide linkage. Signals in the δ 3.0-4.5 ppm region may be due to the methylene (–CH_2–) protons of the Mannich bridge, affirming the formation of C–N–C linkage. The signals of the aliphatic protons are observed in the range of δ 1.0-3.0 ppm.

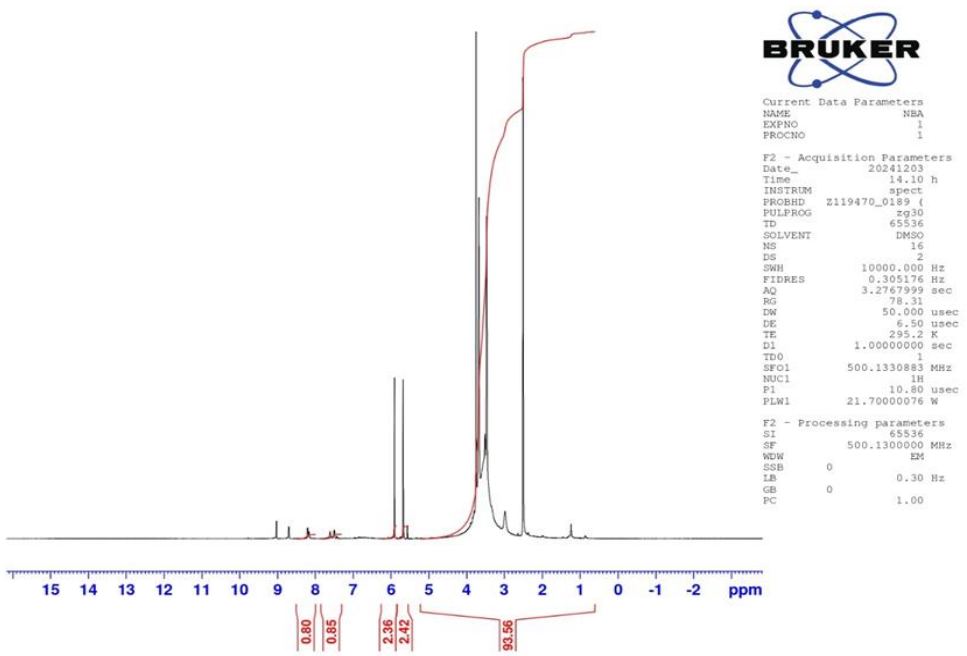

ng

Figure 4. ^1H NMR Spectrum of MVN

The ^{13}C NMR spectrum (Figure 5) also clearly supports the structure, depicting the signals at δ 160-180, δ 120-150 and δ 50-70 ppm with respect to the carbonyl carbons, the aromatic carbons, and for the methylene carbons connected to the nitrogen. Formation of the Mannich base and the conservation of both the carbonyl and aromatic functionalities are hence confirmed.

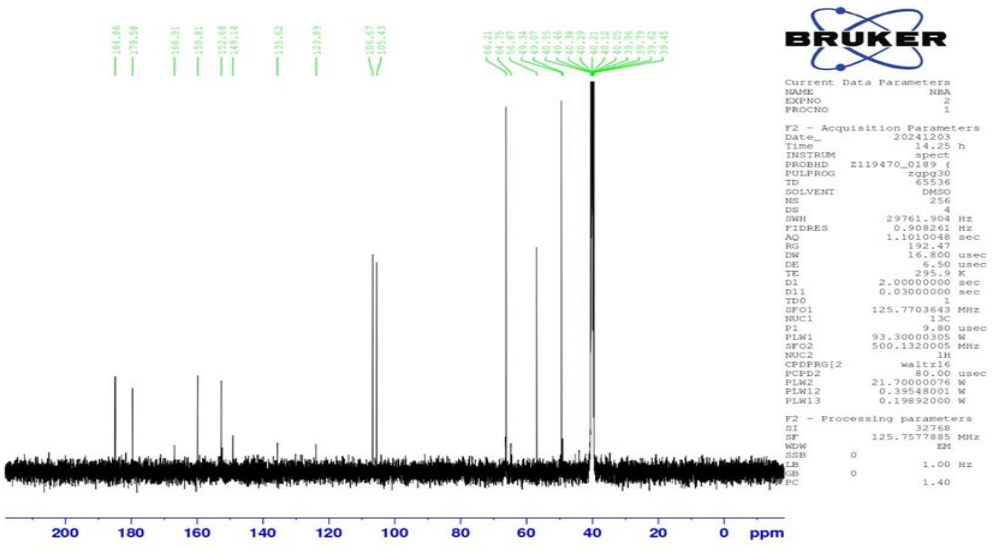

Figure 5. ^{13}C NMR Spectrum of MVN

3.1.4 Mass Spectral Analysis

The mass spectrum (Figure 6) shows the molecular ion peak at m/z 418, for the molecular formula $C_{24}H_{22}N_2O_5$. The appearance of the isotopic peaks at m/z 419 and 420 is consistent with natural isotopic abundance. The stability of the molecular ion peak and the observed fragmentation pattern support the proposed structure of MVN.

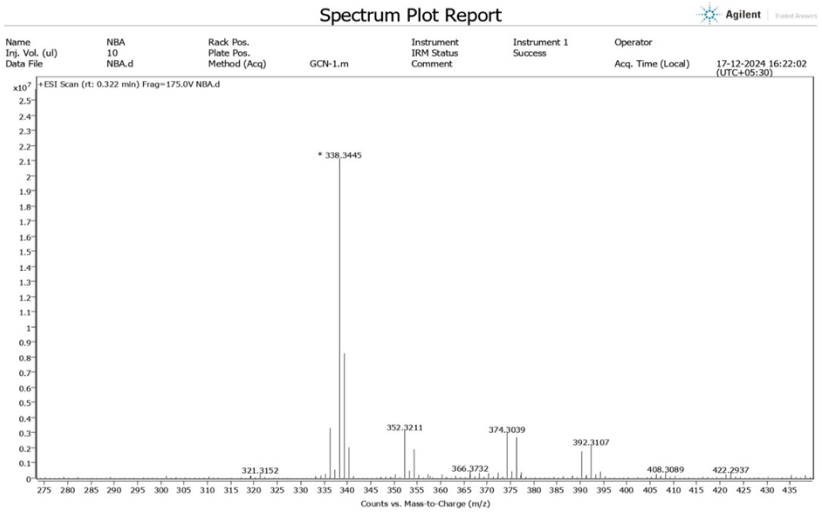

Figure 6. Mass Spectrum of MVN

3.2 Corrosion Inhibition Studies

3.2.1 Weight Loss Measurements

Weight loss investigations shows that the inhibition efficiency of MVN increases as concentration of 1.0 M HCl increases. At 10^{-3} M, the inhibitor conveys a maximum efficiency of 95% (Table 1). The decrease in the rate of corrosion is due to the adsorption of MVN molecules over the surface of the mild steel, creating a protective barrier that restricts metallic dissolution. The increasing inhibition efficiency is attributed to the availability of π-electrons and the heteroatoms (N and O), enhancing adsorption through donor-acceptor interactions with the metal surface.

Table 1 - Corrosion rate, inhibition efficiency and surface coverage of mild steel in 1.0 M HCl for various concentrations of MVN at 303 ± 1 K

S. No	Concentration of Inhibitor (M)	Weight Loss (g)	Corrosion Rate (mpy)	Inhibition Efficiency (%)	Surface Coverage (θ)
1	Blank	0.020	0.0020	-	-
2	0.000001	0.013	0.0013	35.00	0.3500
3	0.00001	0.008	0.0008	60.00	0.6000
4	0.0001	0.004	0.0004	80.00	0.8000
5	0.001	0.001	0.0001	95.00	0.9500

3.2.2 Adsorption Isotherm and Thermodynamic Parameters

The adsorption behavior follows Temkin's adsorption isotherm (Figure 7), shown by the linear relationship between surface coverage (θ) and log C ($R^2 \approx 0.99$). The calculated standard free energy of adsorption ($\Delta G°_{ads} = -34.37$ kJ mol^{-1}) confirms spontaneous adsorption process as it is in between -20 kJ/mol and -40 kJ/mol.

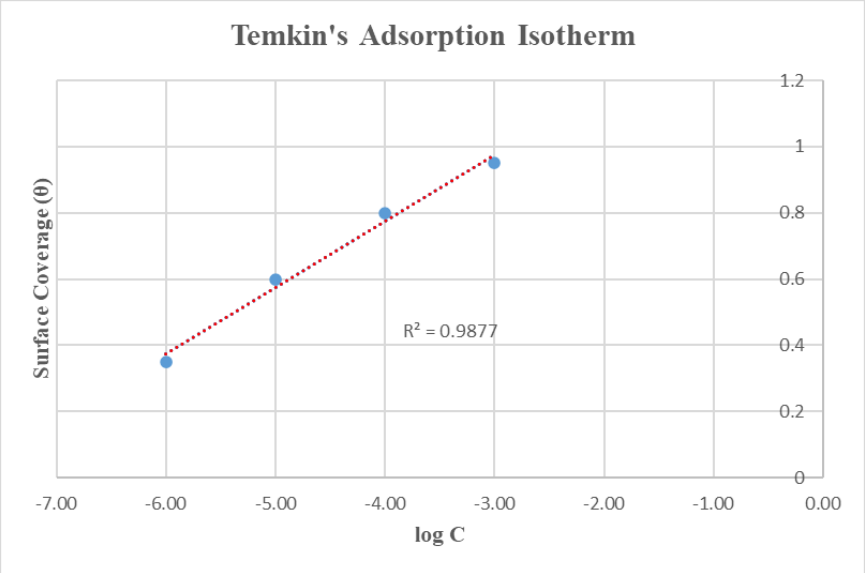

Figure 7. Temkin's Adsorption Isotherm

The magnitude of $\Delta G°_{ads}$ tells that the adsorption process may involve both physisorption and chemisorption, while the chemisorption predominates as there exists a strong interaction between the metal surface and the inhibitor molecules.

3.2.3 Potentiodynamic Polarization Studies

Polarization studies (Figure 8) show a significant decrease in corrosion current density (I_{corr}) in the presence of MVN compared to the blank solution, indicating effective corrosion inhibition (Table 2). The slight shift in corrosion potential (E_{corr}) suggests that MVN acts as a mixed-type inhibitor, affecting both anodic and cathodic reactions. The reduction in I_{corr} confirms the formation of a protective film on the metal surface, which suppresses the corrosion process. The lower value of 0.171762 µA, suggests significantly better corrosion resistance. The increased anodic Tafel slope (b_a) indicates a substantial difference in electrochemical kinetics. Similarly, the difference in the cathodic slope (b_c) signals a completely different cathodic reaction mechanism.

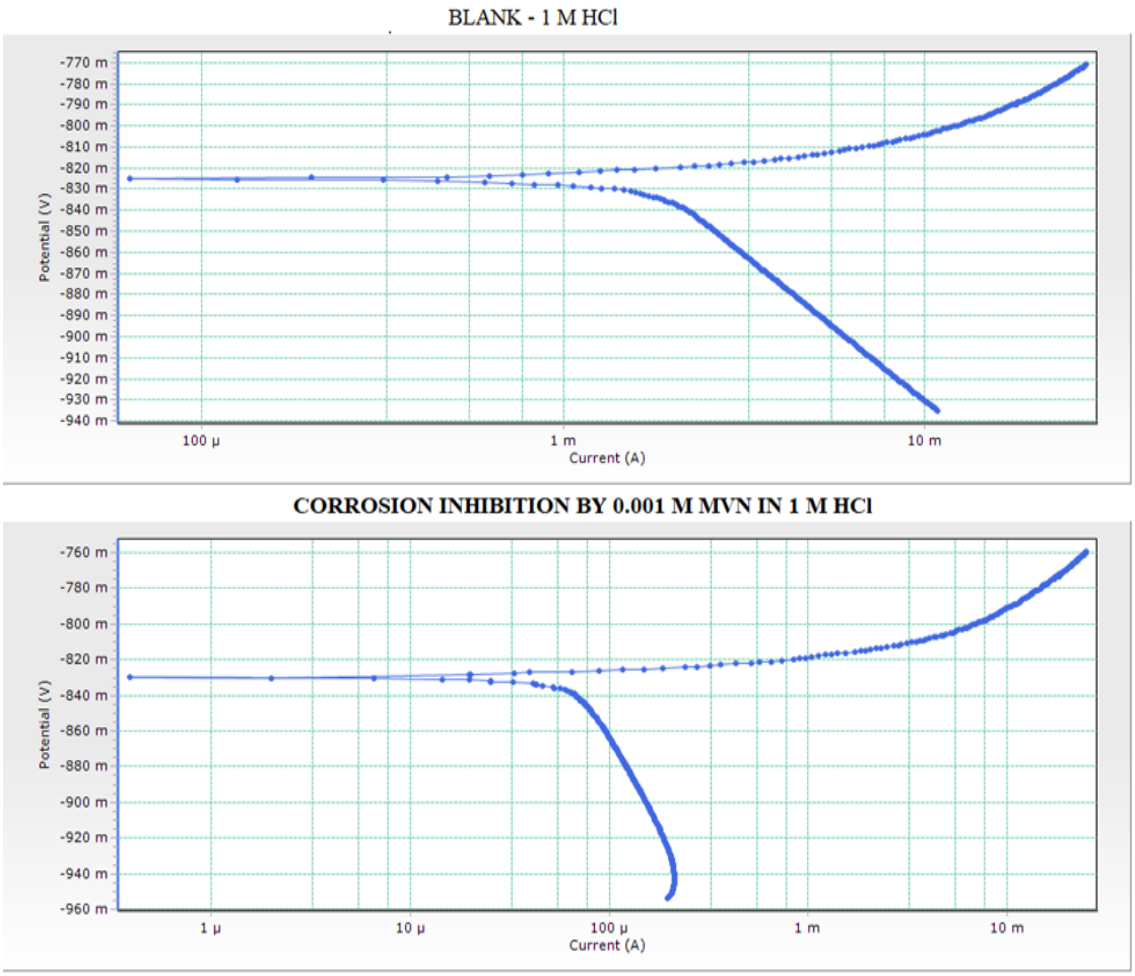

Figure 8. Potentiodynamic Polarization Studies

Table 2 - Electrochemical Parameters for blank and 0.001 M MVN

Sample	**E_{corr} (mV)**	**I_{corr} (mA/µA)**	**b_a (mV/kV)**	**b_c (mV)**
Blank	-825.387	3.149 mA	45.002 mV	254.129 mV
0.001 M MVN	-829.975	0.171762 µA	40.929 kV	-90.462 mV

3.2.4 Electrochemical Impedance Spectroscopy (EIS)

Nyquist plots (Figure 9 & Figure10) exhibit an increase in charge transfer resistance (Rct) with increasing inhibitor concentration, indicating enhanced corrosion resistance (Table 3). Simultaneously, the double layer capacitance (Cdl) decreases, suggesting the formation of an adsorbed protective layer on the metal surface. The increase in semicircle diameter in the presence of MVN confirms improved surface coverage and inhibition efficiency, with maximum protection observed at higher concentrations.

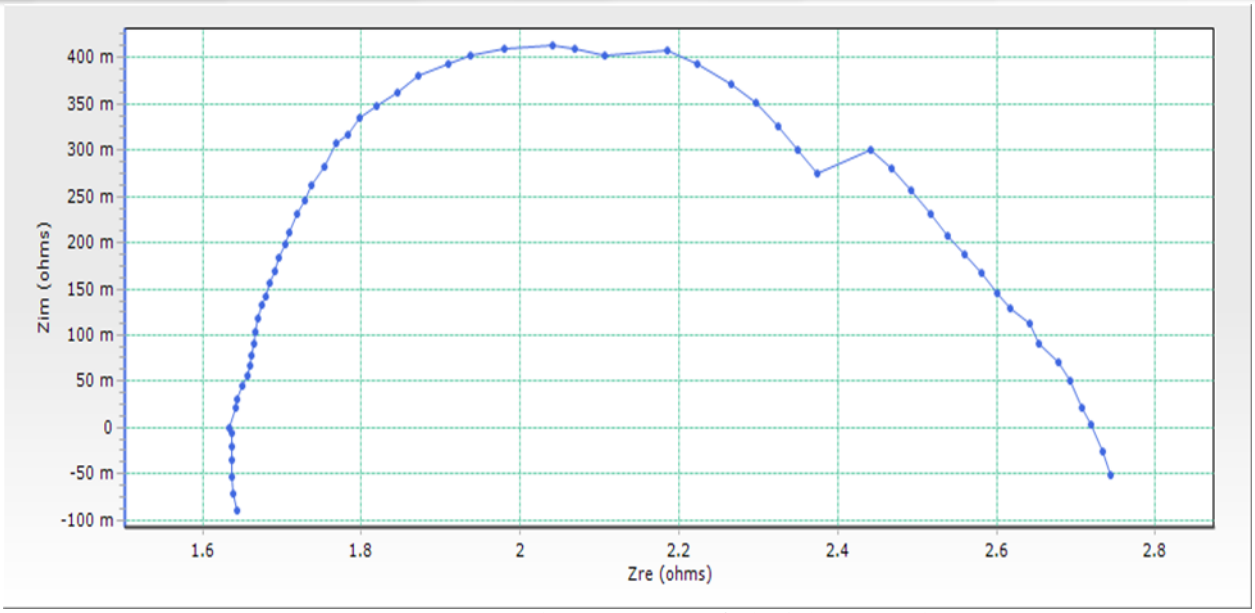

Figure 9. AC- Impedance Spectrum of Blank (1.0 M HCl)

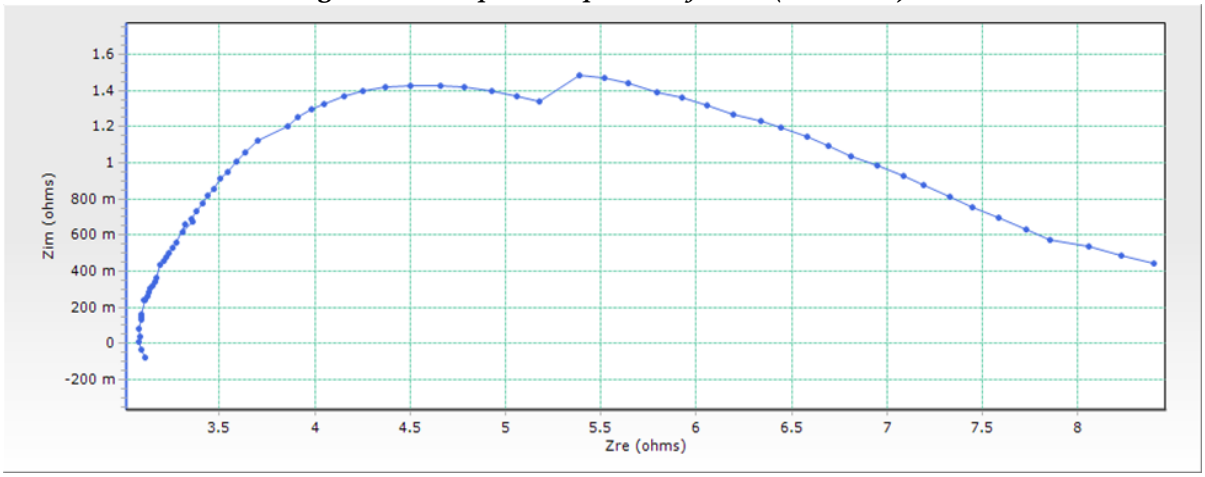

Figure 10. AC- Impedance Spectrum of 0.001 M MVN in I.0 M HCl

Table 3 - Electrochemical Parameters and Corrosion Inhibition Efficiency

Sample Concentrations (M)	Rct (Ω)	Fmax (Hz)	Cdl (F)	I.E. %
Blank	0.94788	69183.09375	2.43×10^{-6}	-
0.001	4.7434	75857.7578125	4.42×10^{-7}	80.02%

1.3 Density Functional Theory (DFT) Studies

1.3.1 Frontier Molecular Orbital (FMO) Analysis

The frontier molecular orbitals (HOMO and LUMO) of MVN are given in Figure 11 and Figure 12. The HOMO is primarily around the aromatic ring and heteroatom-containing regions (nitrogen and oxygen atoms), proposing that these sites are the reason for the electron donation to the metal surface. Such localization increments the adsorption potentials of the molecule through coordination with the vacant d-orbitals.

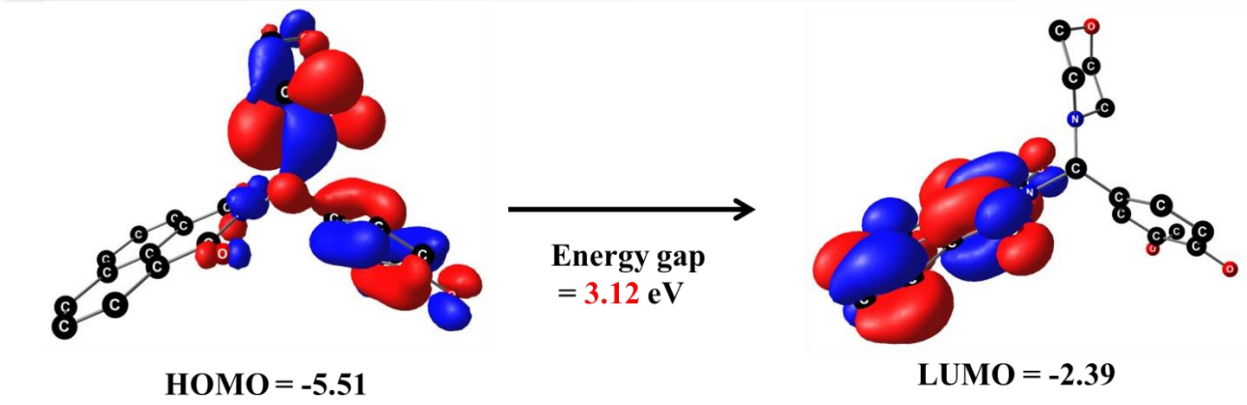

Figure 11. Optimized structure and FMO orbitals of MVN.

The LUMO is delocalized over the conjugated molecular framework, confirming the capability of MVN to accept electrons from the metal surface. This approves a feedback interaction mechanism, increasing the strength of the adsorption process. The quantum chemical parameters are calculated as: E_{HOMO} = −5.51 eV; E_{LUMO} = −2.39 eV; ΔE = 3.12 eV.

A relatively high HOMO energy (less negative value) shows enhanced electron-donating potential of MVN, promoting chemisorption onto the metal surface. The LUMO energy conveys favorable tendency to accept electrons, further stabilizing the adsorption process. As the energy gap (ΔE = 3.12 eV) is low, higher molecular reactivity and an increased adsorption efficiency is proposed. In general, the molecules with lesser energy gaps are greater corrosion inhibitors owing to their interactive ability with the metal surface.

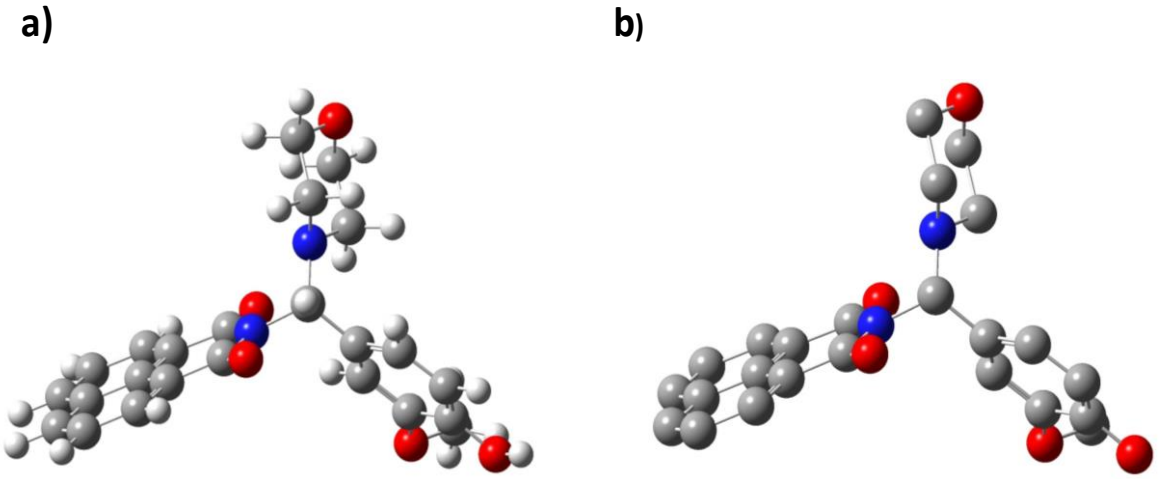

Figure 12. Computed Optimized structure

3.3.2 Molecular Electrostatic Potential (MEP) Analysis

The molecular electrostatic potential (MEP) surface of MVN (Figure 13) shows the charge distribution, where red regions give the electron-rich sites and blue regions foretells the electron-deficient areas. The greatly negative potential is predominately localized around oxygen and nitrogen atoms, signalling them as active sites for interaction with the metal surface through donor-acceptor mechanisms (Moradi et al., 2011).

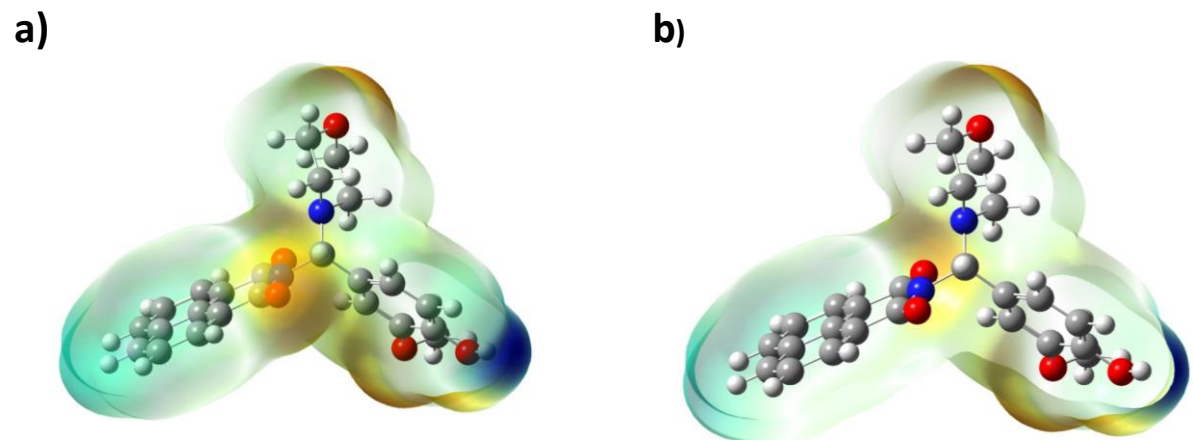

Figure 13. Molecular electrostatic potential (MESP) energy surface of MVN

The occurrence of electron-rich regions and delocalized π-electrons implies a stronger adsorption of MVN onto the mild steel surface via both chemisorption and physisorption processes (Peter et al., 2015). This facilitates the formation of a stable protective film, thereby comprehending corrosion inhibition efficiency. The MEP results are consistent with DFT and experimental findings, confirming the role of heteroatoms and conjugation in improving inhibition performance (Politzer & Murray, 2002).

3.3.3 Global Reactivity Parameters and Corrosion Inhibition

The quantum chemical parameters derived from E_{HOMO} and E_{LUMO} provide further insight into the inhibition mechanism. The relatively small energy gap helps the electron transfer between MVN molecule and the metal surface, increasing the adsorption strength.

The availability of multiple adsorption centres, like the nitrogen and oxygen atoms as well as π-electrons of aromatic rings, contributes greatly towards the inhibition efficiency. These active sites enable the electron donation to metal (chemisorption), the back-donation from metal (feedback bonding), and the electrostatic interactions (physisorption). All these effects together lead to the formation of a stable protective film on the mild steel surface, which is consistent with the experimentally observed high inhibition efficiency (95%).

The moderate energy gap, favorable HOMO–LUMO distribution, and presence of electron-rich centres enhance adsorption of the inhibitor onto the mild steel surface together results in a decrease in corrosion current density, increase in charge transfer resistance, and the formation of a compact protective layer. The theoretical results validate the experimental conclusion that the synthesized MVN acts as an efficient corrosion inhibitor in acidic medium.

3.4 Mechanism of Corrosion Inhibition

The inhibition of mild steel corrosion by MVN in 1.0 M HCl is primarily attributed to adsorption at the metal/solution interface. The adsorption occurs through multiple interactions: (i) electrostatic attraction between charged species, (ii) coordination between lone pair electrons of heteroatoms (N and O) and the metal surface, and (iii) interaction of π-electrons from aromatic rings with the d-orbitals of iron.

The presence of functional groups such as –NH–C=O, heterocyclic nitrogen, and aromatic rings enhance adsorption strength. The combined effect of physisorption and chemisorption leads to the formation of a stable protective film, thereby reducing the corrosion rate. This mixed adsorption mechanism accounts for the high inhibition efficiency of MVN in acidic medium.

CONCLUSION

A novel Mannich base, 2-[(4-hydroxy-3-methoxyphenyl)-morpholin-4-yl-methyl]-benzo[de]isoquinoline-1,3-dione (MVN), was successfully synthesized and structurally confirmed through UV–Visible, FT–IR, NMR, and mass spectral analyses. The combined spectroscopic evidence established the presence of key functional groups, conjugated aromatic systems, and the characteristic C–N–C linkage of the Mannich framework, validating the proposed molecular structure.

Corrosion inhibition studies demonstrated that MVN exhibits excellent inhibitory performance for mild steel in 1.0 M HCl, achieving a maximum efficiency of 95% at 10^{-3} M concentration. Gravimetric and electrochemical results consistently revealed a significant reduction in corrosion rate, decrease in corrosion current density, and increase in charge transfer resistance, indicating the formation of a stable

and protective adsorbed film on the metal surface.

Adsorption studies showed that the inhibition process follows Temkin's isotherm, with a negative free energy of adsorption ($\Delta G°_{ads} = -34.37$ kJ mol^{-1}), confirming a spontaneous process involving both physisorption and chemisorption. The high inhibition efficiency is attributed to the synergistic effect of heteroatoms (N and O), π-electron density, and the presence of multiple adsorption centers within the MVN molecule, which facilitate strong interaction with the metal surface.

DFT results confirm that MVN exhibits strong adsorption ability. The moderate energy gap (3.12 eV) and electron-rich N and O atoms enhance interaction with the metal surface, supporting its high inhibition efficiency.

Overall, MVN acts as an efficient mixed-type corrosion inhibitor, suppressing both anodic and cathodic reactions. Its high efficiency, combined with structural features favorable for adsorption, highlights its potential as a promising candidate for corrosion protection in acidic environments. The findings of this study provide valuable insights into the design of new Mannich base inhibitors with enhanced performance and potential industrial applicability.

BIBLIOGRAPHY

1. Al-Amiery, A. A., Mohamad, A. B., Kadhum, A. A. H., Shaker, L. M., Isahak, W. N. R. W., & Takriff, M. S. (2022). Experimental and theoretical study on the corrosion inhibition of mild steel by nonanedioic acid derivative in hydrochloric acid solution. Scientific Reports, 12(1), 4705.
2. Bentiss, F., Traisnel, M., & Lagrenee, M. (2000). The substituted 1, 3, 4-oxadiazoles: a new class of corrosion inhibitors of mild steel in acidic media. Corrosion science, 42(1), 127-146.
3. BRIAN S FURNIS, F. (2020). VOGEL'S TEXTBOOK OF PRACTICAL ORGANIC CHEMISTRY. In: LONGMAN SCIENTIFIC AND TECHNICAL.
4. Dwivedi, A., Bharti, P., & Shukla, S. K. (2021). An overview of the polymeric materials that can be used to prevent metal corrosion: a review. Journal of the Turkish Chemical Society Section A: Chemistry, 8(3), 863-872.
5. Ebenso, E. (2003). Synergistic effect of halide ions on the corrosion inhibition of aluminium in H2SO4 using 2-acetylphenothiazine. Materials Chemistry and Physics, 79(1), 58-70.
6. Eddy, N., Odoemelam, S., Ogoko, E., & Ita, B. (2010). Inhibition of the Corrosion of Zinc in 0.01-0.04 M H2SO4 by Erythromycin. Portugaliae Electrochimica Acta, 28(1), 15-26.
7. El Ibrahimi, B., & Berdimurodov, E. (2023). Weight loss technique for corrosion measurements. In Electrochemical and analytical techniques for sustainable corrosion monitoring (pp. 81-90). Elsevier.
8. Elachouri, M., Hajji, M., Salem, M., Kertit, S., Aride, J., Coudert, R., & Essassi, E. (1996). Some nonionic surfactants as inhibitors of the corrosion of iron in acid chloride solutions. Corrosion, 52(2), 103-108.
9. Emmanuel, J. K. (2024). Corrosion protection of mild steel in corrosive media, a shift from synthetic to natural corrosion inhibitors: a review. Bulletin of the National Research Centre, 48(1), 26.
10. Evans, J. W., & Kim, S.-w. (2001). Elements of Corrosion. In Product Integrity and Reliability in Design (pp. 178-203). Springer.
11. Jones, D. A. (1996). Principles and prevention of corrosion. (No Title).
12. Ju, H., Kai, Z.-P., & Li, Y. (2008). Aminic nitrogen-bearing polydentate Schiff base compounds as corrosion inhibitors for iron in acidic media: a quantum chemical calculation. Corrosion Science, 50(3), 865-871.
13. Koch, G. H., Brongers, M. P., Thompson, N. G., Virmani, Y. P., & Payer, J. H. (2005). Cost of corrosion in the United States. In Handbook of environmental degradation of materials (pp. 3-24). Elsevier.
14. Kumar, A., Thakur, A., & Ebenso, E. E. (2024). Corrosion inhibition-recent advancements. In (Vol. 12, pp. 1493419): Frontiers Media SA.
15. Langmuir, I. (1918). The adsorption of gases on plane surfaces of glass, mica and platinum. Journal of the American Chemical society, 40(9), 1361-1403.
16. Liu, J., Hou, Z., Cao, J., & Liu, J. (2026). Corrosion inhibition of a Mannich base on N80 steel in a 20% HCl solution. Canadian Metallurgical Quarterly, 65(2), 1743-1752.
17. Macdonald, D. D. (2006). Reflections on the history of electrochemical impedance spectroscopy. Electrochimica acta, 51(8-9), 1376-1388.
18. Mansfeld, F. (1990). Electrochemical impedance spectroscopy (EIS) as a new tool for investigating methods of corrosion protection. Electrochimica Acta, 35(10), 1533-1544.
19. Mobin, M., Zamindar, S., & Banerjee, P. (2023). Mechanistic insight into adsorption and anti-corrosion capability of a novel surfactant-derived ionic liquid for mild steel in HCl medium. Journal of Molecular Liquids, 385, 122403.
20. Moradi, M., Duan, J., Ashassi-Sorkhabi, H., & Luan, X. (2011). De-alloying of 316 stainless steel in the presence of a mixture of metal-oxidizing bacteria. Corrosion science, 53(12), 4282-4290.
21. Pavia, D. L., Lampman, G. M., Kriz, G. S., & Vyvyan, J. R. (2001). Introduction to

spectroscopy. Belmont, USA, 13.
22. Pedeferri, P. (2018). High temperature corrosion. In Corrosion Science and Engineering (pp. 589-610). Springer.
23. Peter, A., Obot, I., & Sharma, S. K. (2015). Use of natural gums as green corrosion inhibitors: an overview. International Journal of Industrial Chemistry, 6(3), 153-164.
24. Politzer, P., & Murray, J. S. (2002). The fundamental nature and role of the electrostatic potential in atoms and molecules. Theoretical Chemistry Accounts, 108(3), 134-142.
25. Popova, A. (2007). Temperature effect on mild steel corrosion in acid media in presence of azoles. Corrosion science, 49(5), 2144-2158.
26. Quraishi, M., & Jamal, D. (2001). Corrosion inhibition by fatty acid oxadiazoles for oil well steel (N-80) and mild steel. Materials chemistry and physics, 71(2), 202-205.
27. Quraishi, M., & Rawat, J. (2001). Influence of iodide ions on inhibitive performance of tetraphenyl-dithia-octaaza-cyclotetradeca-hexaene (PTAT) during pickling of mild steel in hot sulfuric acid. Materials Chemistry and Physics, 70(1), 95-99.
28. Raja, P. B., & Sethuraman, M. G. (2008). Natural products as corrosion inhibitor for metals in corrosive media—a review. Materials letters, 62(1), 113-116.
29. Silverstein, R., Bassler, G., & Morril, T. (2005). Spectrometric Identification of Organic Compounds. 7th Edn. N. In: John Wiley & Sons, New York), I.
30. Singh, A. K., & Quraishi, M. (2010). Effect of Cefazolin on the corrosion of mild steel in HCl solution. Corrosion Science, 52(1), 152-160.
31. Skoog, D. A., Holler, F. J., & Crouch, S. (2007). Principles of instrumental analysis. Thomson Brooks. Cole, Canada.
32. Smith, M. B. (2025). March's advanced organic chemistry: reactions, mechanisms, and structure. John Wiley & Sons.
33. Stern, M., & Geary, A. L. (1957). Electrochemical polarization: I. A theoretical analysis of the shape of polarization curves. Journal of the electrochemical society, 104(1), 56-63.
34. Verma, C., Ebenso, E. E., Vishal, Y., & Quraishi, M. (2016). Dendrimers: a new class of corrosion inhibitors for mild steel in 1 M HCl: experimental and quantum chemical studies. Journal of Molecular Liquids, 224, 1282-1293.
35. Watson, J. T., & Sparkman, O. D. (2007). Introduction to mass spectrometry: instrumentation, applications, and strategies for data interpretation. John Wiley & Sons.

